

Particle-hole induced intruder bands in ^{117}Sb and ^{119}Sb

D. R. LaFosse,* D. B. Fossan, J. R. Hughes,† Y. Liang,‡ H. Schnare,§ P. Vaska, M. P. Waring, and J.-y. Zhang||
Department of Physics, State University of New York at Stony Brook, Stony Brook, New York 11794

(Received 16 December 1996)

Collective structures have been investigated via γ -ray studies in $^{117,119}\text{Sb}$. Previously observed strongly coupled $(\pi g_{9/2})^{-1}$ bands in both nuclei involving 1p-1h proton excitations across the $Z=50$ gap have been extended, and an alignment of $h_{11/2}$ neutrons identified. New negative-parity strongly coupled bands based on this proton configuration have also been observed in both nuclei. Decoupled bands involving 2p-2h excitations across the gap have been observed in ^{119}Sb , similar to those presented earlier for ^{117}Sb . These bands are interpreted as due to the coupling of a low- K valence proton to the $(\pi g_{7/2}d_{5/2})^2 \otimes (\pi g_{9/2})^{-2}$ deformed state of the respective $_{50}\text{Sn}$ core nuclei. Anomalies in the expected $h_{11/2}$ neutron crossing of these bands are discussed. [S0556-2813(97)06308-5]

PACS number(s): 21.10.Re, 27.70.+q, 23.20.Lv.

I. INTRODUCTION

The structure of high-spin states in neutron deficient nuclei near the $Z=50$ major shell closure has recently provided a wealth of interesting physics. Nuclei near this closed proton shell exhibit a variety of collective structures that coexist with the expected single-particle structure. Collectivity in the $Z=50$ region was initially observed in the $Z=51$ odd- A Sb isotopes [1,2], which involved 1p-1h excitations across the shell gap making deformed 2p1h proton configurations, with the β -upsloping $\pi g_{9/2}$ orbital intruding from below the $Z=50$ proton shell. These high- K $9/2^+$ states $\pi(g_{7/2}d_{5/2})^2(g_{9/2})^{-1}$ of modest prolate deformation give rise to strongly coupled ($\Delta I=1$) rotational bands. Subsequently, related deformed 2p-2h excitations, $\pi(g_{7/2}d_{5/2})^2(g_{9/2})^{-2}$, were discovered via rotational bands in the even- A Sn isotopes [3], which achieved the lowest energy in ^{116}Sn near the neutron midshell. An investigation in ^{117}Sb [4], representing the initial phase of the current work, revealed collective structure in odd- A $Z=51$ Sb nuclei, that involved the coupling of these 2p-2h Sn-core deformed states to the low- K valence $d_{5/2}$, $g_{7/2}$, and $h_{11/2}$ proton orbitals above the gap. In ^{113}Sb [5] the yrast band based on the $\pi h_{11/2}$ orbital and the 2p-2h deformed core was observed to $75/2\hbar$ with an enhanced quadrupole deformation, $\beta_2 \approx 0.3$.

New physics in this $Z=50$ region regarding these collective structures has been recently demonstrated in several $Z=51$ [6–9,5,10] and $Z=50$ [11–13] nuclei. Intruder bands in these nuclei based on 2p-2h excitations across the shell

gap were observed to extremely high frequency approaching $\hbar\omega=1.5$ MeV with gradually decreasing dynamic moments of inertia ($\mathcal{J}^{(2)}$) to values well below the rigid body moment of inertia. The unique features of these intruder bands have been interpreted as “soft band termination” in terms of the configuration dependent cranked shell model [14,15].

Since the high-spin terminating bands in the Sb isotopes all have configurations involving the 2p-2h proton excitation across the $Z=50$ gap, a study of the formation of these Sb bands beyond the neutron midshell, where the 2p-2h Sn-core states have the lowest energy relative to the spherical ground states, should provide further information about the lower spin properties of these interesting collective structures. For this reason, the ^{117}Sb and ^{119}Sb isotopes at $N=66$ and 68 , respectively, have been studied and are the focus of this work. Along with new results for the ^{115}Sb nucleus [16,17] at $N=64$, these Sb intruder bands will have been followed from $N=58$ to 68 for the systematic investigation of the $Z=51$ collective properties. These heavier Sb nuclei cannot be populated to spins approaching termination, due to the restrictive target-beam combinations available; thus, the configuration dependent cranked shell model is not applicable, as this model does not include pairing correlations present at moderate spins.

II. EXPERIMENTAL DETAILS

High spin states in $^{117,119}\text{Sb}$ were studied via heavy ion fusion-evaporation reactions with beams provided by the Stony Brook superconducting LINAC facility. The ^{110}Pd ($^{11}\text{B},4n$) reaction with a 45-MeV beam was employed to populate ^{117}Sb . The target consisted of 2.9 mg/cm^2 ^{110}Pd , backed with ^{208}Pb sufficient to stop the recoiling residual nuclei. The nucleus ^{119}Sb was studied via the $^{116}\text{Cd}(^7\text{Li},4n)$ reaction with a 35-MeV beam. The target for this experiment was 3.2 mg/cm^2 thick and also backed with ^{208}Pb . The γ rays emitted by the excited residual nuclei were detected with six Compton-suppressed high-purity Ge detectors, each possessing a relative efficiency of approximately 25%. A cluster of seven hexagonal close-packed BGO detectors was placed above the target chamber and a second similar cluster below; these detectors covered 80% of 4π and

*Current address: Chemistry Department, Washington University, St. Louis, MO 63130.

†Current address: Lawrence Livermore Laboratory, P.O. Box 808, Livermore, CA 94550.

‡Current address: I.U.P.U. I., Indianapolis, IN 46202.

§Current address: Research Center Rossendorf, PF 510119, D-01314 Dresden, Germany.

||Current address: University of Tennessee, Knoxville TN 37796; permanent address: Institute of Modern Physics, Lanzhou, P.R. China.

were used as a multiplicity filter. The event trigger required that two or more Ge detectors and two or more BGO elements detect a signal within a $2\tau=100$ ns coincidence time window. Events meeting this criterion were then recorded onto magnetic tape for subsequent off-line analysis. In this manner, over 6.2×10^7 events were collected during the ^{117}Sb experiment, and over 5.5×10^7 events for the ^{119}Sb experiment.

In order to facilitate the extraction of coincidence relationships between γ rays, the coincidence data were then sorted off line into $2k$ by $2k$ $E_\gamma - E_\gamma$ matrices. The multiplicities of the transitions were determined via the directional correlation (DCO) method [18]. In this type of analysis, an asymmetric $E_\gamma - E_\gamma$ matrix is created by sorting detectors placed at angles near 90° against the remaining forward-backward detectors. With gates on known $E2$ transitions on both axes of this matrix, the measured intensity ratios yield information on the multipolarity of the transitions. The DCO ratios were calibrated using transitions with known multipolarity in nuclei populated in the two experiments. Thus it was determined that with an $E2$ gating transition, a DCO ratio of ~ 1.0 indicated a stretched quadrupole transition, while a DCO ratio of ~ 0.5 indicated a dipole transition. The Radware software package [19] was used for all the data analysis.

III. EXPERIMENTAL RESULTS

The level schemes for ^{117}Sb and ^{119}Sb were constructed from the coincidence data. The placement of transitions was determined through a combination of γ -ray coincidence relationships, intensity balances, and energy sums. The level schemes for ^{117}Sb and ^{119}Sb are shown in Fig. 1. Tables I and II report the energies, initial and final spin states, DCO ratios, and multiplicities of all the transitions identified in ^{117}Sb and ^{119}Sb , respectively. The two level schemes will be discussed further in the following subsections.

A. The level scheme of ^{117}Sb

Low-spin levels in ^{117}Sb had previously been identified in several studies [1,2,20]. These studies uncovered a number of spherical levels of multiquasiparticle nature, and a single strongly coupled rotational band. The current work has uncovered many new spherical levels, as well as four additional rotational structures. The new rotational structures have been previously reported in Ref. [4].

Band 5a is a strongly coupled structure, composed of two bands of opposite signature connected by strong $M1/E2$ transitions, as determined through DCO measurements. A spectrum obtained from a gate on the 465-keV transition of this band can be seen in Fig. 2. This structure was populated with $\sim 22\%$ of the reaction channel cross section. The band had been previously observed from the $J^\pi=9/2^+$ bandhead to the $J^\pi=17/2^+$ state [2], but has been extended up to $J^\pi=(27/2^+)$ in this study.

A short sequence of transitions was observed to feed into band 5a at the $23/2^+$ and $21/2^+$ band members. This sequence is labeled band 5b in Fig. 1. Due to the low intensities with which several of these transitions were observed, DCO analysis was not always possible; thus the spins and

parities of the upper members are unknown. It was possible to obtain a DCO ratio for the 423-keV transition connecting the $25/2^+$ state of band 5b to the $23/2^+$ state of band 5a; the DCO ratio was found to be 0.78 ± 0.18 , consistent with a mixed $M1/E2$ character. This fixes both the spin and parity of the $25/2^+$ state of band 5b. The energies of the higher transitions of band 5b suggest that these transitions are also of mixed $M1/E2$ dipole character. With these assignments, this sequence extends up to $J^\pi=(33/2^+)$.

Band 4 is a second strongly coupled structure, populated with $\sim 9\%$ of the reaction channel intensity. It had not been reported prior to this study. This strongly coupled band was found to be built on a $J^\pi=23/2^-$ state, which is a known $t_{1/2}=290$ ns isomer [20] (labeled in Fig. 1). The lifetime of this state is long enough to significantly reduce the coincidence intensity between transitions above and below the isomer. This, however, does not undermine the assignment of this band to ^{117}Sb , as the band was observed to be in weak coincidence with transitions below the isomer, and was determined not to be in coincidence with strong transitions in other nuclei populated in this experiment. Interestingly, the quadrupole moment of this isomer has been determined to be $Q=2.46 \pm 25 e b^2$ [21]. This is a significant deformation, and the discovery of a rotational band built on this state is thus reasonable.

Bands 1 and 2 are sequences of stretched $E2$ transitions, which had also not been observed before this study. The bands were observed to have only 1% and 2.5%, respectively, of the total intensity of the ^{117}Sb channel in this experiment. The spins and parities of these bands were determined through the DCO ratios of the transitions which depopulate the bottom levels of the bands. Thus, band 1 was found to initiate from $J^\pi=15/2^+$ and extends to $J^\pi=(35/2^+)$; band 2 begins at $13/2^+$ and extends to $(41/2^+)$. Band 1 is observed to decay predominantly into two $11/2^+$ states, and then to the $7/2^+$ state. Band 2 decays to at least two states having $J^\pi=9/2^+$ (a third state populated by this band has unknown spin) and then the most intense decay path flows directly to the $5/2^+$ ground state.

Band 3 was the most strongly populated of the decoupled bands, having been observed with 7% of the reaction channel intensity. The band originates from $J^\pi=19/2^-$ and extends to $J^\pi=(43/2^-)$. This band is observed to decay into two $15/2^-$ states, the majority of the decay feeding into the highest-lying of these states at 2413 keV; both then decay exclusively into the $11/2^-$ state at 1323 keV. A spectrum representing this band can be seen in Fig. 3.

A final interesting sequence is the 705-776-842 series of transitions, labeled band 1a in Fig. 1. Only one transition was observed to depopulate this sequence; it was found to have a DCO ratio of 0.93 ± 0.20 . This value is suggestive of a stretched $E2$ transition, however a dipole or nonstretched $E2$ transition cannot be ruled out due to the large uncertainty. Unfortunately the low intensities of the transitions in this sequence prevented the extraction of DCO ratios and thus their multiplicities are unknown.

Finally, two of the transitions shown in Fig. 1 were not observed in this experiment. They are the $11/2^- - 9/2^+$ 12-keV transition and the $23/2^- - 19/2^-$ 16-keV transition. The first was reported in Ref. [2], but could be inferred in this study from coincidence relationships. The second of

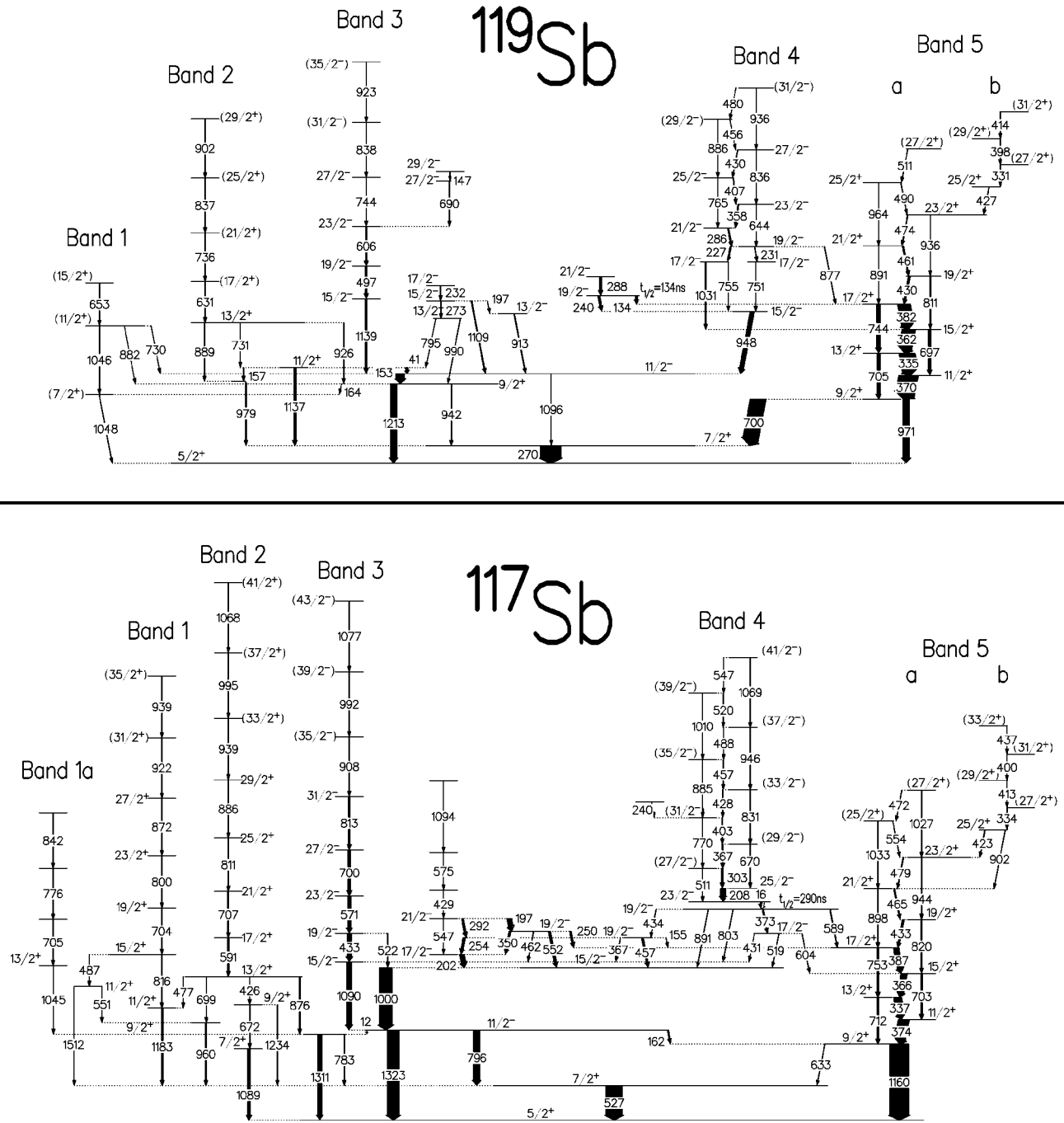


FIG. 1. The level schemes of ^{119}Sb (top) and ^{117}Sb (bottom) extracted for this investigation. Gamma-ray energies are given in keV, and the widths of the arrows represents relative intensities. Previously known isomers are labeled in the figure with their half-lives.

these transitions depopulates the $J^\pi=23/2^-$ isomer as reported in Ref. [20].

B. ^{119}Sb

The low-spin levels of ^{119}Sb had also been studied prior to this work [1,2]. These investigations uncovered several spherical levels, a strongly coupled band extending to $J^\pi=17/2^+$ and a $t_{1/2}=128\text{ ns}$ isomer [22]. This isomeric state is labeled in Fig. 1.

As was the case for ^{117}Sb , the present work greatly expands on the previous studies. In addition to the discovery of many new presumably spherical states, the aforemen-

tioned strongly coupled rotational band was extended to $J^\pi=(27/2^+)$. This structure is labeled band 5a in Fig. 1, and can be seen in Fig. 2. The band was populated with approximately 45% of the $4n$ reaction channel intensity in this experiment. A short sequence of low energy transitions, labeled band 5b, was observed to feed into this band at the $J^\pi=23/2^+$ level. Similar to band 5b in ^{117}Sb , the DCO ratio of the 427-keV transition linking bands 5a and 5b strongly implies a spin and parity of $25/2^+$ for the bottom member of band 5b. The remaining higher-lying transitions are presumed to be of mixed $M1/E2$ character; however, the low intensity of these transitions did not permit the extraction of

TABLE I. Table giving information on transitions assigned to ^{117}Sb .

Energy, keV ^a	$I_i^\pi - I_f^\pi$	Intensity ^b	DCO ratio	Multipolarity
12.3	$11/2^- - 9/2^+$	c	c	$E1^f$
16.4	$23/2^- - 19/2^-$	d	d	$E2^g$
154.8	$19/2^- - 17/2^+$	<2	e	$E1$
162.3	$11/2^- - 9/2^+$	6(1)	e	$E1^f$
196.9	$21/2^- - 19/2^-$	23(1)	0.50 ± 0.05	$M1/E2$
201.7	$17/2^- - 15/2^-$	23(1)	e	$M1/E2^f$
207.6	$25/2^- - 23/2^-$	25(1)	0.58 ± 0.04	$M1/E2$
239.9	$-(31/2^-)$	<2	e	
250.1	$19/2^- - 17/2^+$	9(1)	e	$E1^f$
254.4	$19/2^- - 17/2^-$	12(1)	0.67 ± 0.06	$M1/E2$
292.3	$21/2^- - 19/2^-$	10(1)	0.71 ± 0.07	$M1/E2$
302.8	$(27/2^-) - 25/2^-$	8(1)	e	$(M1/E2)$
334.2	$(27/2^+) - 25/2^+$	3(1)	e	$(M1/E2)$
336.7	$13/2^+ - 11/2^+$	41(2)	1.04 ± 0.05	$M1/E2^f$
349.7	$19/2^- - 17/2^-$	10(1)	e	$M1/E2^f$
365.7	$15/2^+ - 13/2^+$	33(2)	0.99 ± 0.05	$M1/E2^f$
366.6	$(29/2^-) - (27/2^-)$	7(1)	e	$(M1/E2)$
367.3	$19/2^- - 15/2^-$	2(1)	e	$E2$
372.6	$19/2^- - 17/2^-$	6(1)	e	$M1/E2$
374.3	$11/2^+ - 9/2^+$	57(3)	1.05 ± 0.05	$M1/E2^f$
387.0	$17/2^+ - 15/2^+$	29(2)	0.95 ± 0.06	$M1/E2^f$
399.7	$(31/2^+) - (29/2^+)$	<2	e	$(M1/E2)$
402.5	$(31/2^-) - (29/2^-)$	3(1)	e	$(M1/E2)$
413.4	$(29/2^+) - (27/2^+)$	<2	e	$(M1/E2)$
423.2	$25/2^+ - 23/2^+$	3(1)	0.72 ± 0.18	$M1/E2$
425.6	$13/2^+ - 9/2^+$	2(1)	1.26 ± 0.14	$E2$
427.6	$(33/2^-) - (31/2^-)$	2(1)	e	$(M1/E2)$
429.3	$-21/2^-$	2(1)	e	
430.5	$17/2^- - 15/2^-$	<2	e	$M1/E2$
432.7	$19/2^- - 15/2^-$	23(1)	1.18 ± 0.06	$E2$
432.8	$19/2^+ - 17/2^+$	10(1)	0.90 ± 0.24	$M1/E2$
433.5	$19/2^- - 19/2^-$	<2	e	$M1/E2$
437.1	$(33/2^+) - (31/2^+)$	<2	e	$(M1/E2)$
456.8	$19/2^- - 15/2^-$	10(1)	e	$E2^f$
456.9	$(35/2^-) - (33/2^-)$	<2	e	$(M1/E2)$
462.4	$19/2^- - 15/2^-$	2(1)	e	$E2$
464.9	$21/2^+ - 19/2^+$	6(1)	0.77 ± 0.21	$M1/E2$
472.2	$(27/2^+) - (25/2^+)$	<2	e	$(M1/E2)$
476.8	$13/2^+ - 11/2^+$	<2	0.46 ± 0.10	$M1/E2$
478.6	$23/2^+ - 21/2^+$	4(1)	0.65 ± 0.18	$M1/E2$
486.8	$15/2^+ - 11/2^+$	<2	0.98 ± 0.17	$E2$
488.3	$(37/2^-) - (35/2^-)$	<2	e	$(M1/E2)$
511.0	$(27/2^-) - 23/2^-$	<2	e	$(E2)$
518.5	$17/2^- - 15/2^-$	<2	e	$M1/E2^g$
520.3	$(39/2^-) - (37/2^-)$	<2	e	$(M1/E2)$
522.3	$19/2^- - 15/2^-$	2(1)	1.04 ± 0.14	$E2$
527.1	$7/2^+ - 5/2^+$	87(5)	0.64 ± 0.04	$M1/E2$
546.9	$(41/2^-) - (39/2^-)$	<2	e	$(M1/E2)$
547.3	$21/2^- - 17/2^-$	<2	e	$E2$
551.4	$11/2^+ -$	<2	e	
552.0	$19/2^- - 15/2^-$	13(1)	1.13 ± 0.11	$E2$
553.5	$(25/2^+) - 23/2^+$	<2	e	$(M1/E2)$
570.5	$23/2^- - 19/2^-$	19(1)	1.03 ± 0.09	$E2$
574.7		<2	e	
589.3	$19/2^- - 17/2^+$	4(1)	e	$E1^g$

TABLE I. (*Continued.*)

Energy, keV ^a	$I_i^\pi - I_f^\pi$	Intensity ^b	DCO ratio	Multipolarity
591.2	17/2 ⁺ - 13/2 ⁺	7(1)	1.04 ± 0.10	E2
604.0	17/2 ⁻ - 15/2 ⁺	2(1)	^e	E1 [§]
632.6	9/2 ⁺ - 7/2 ⁺	2(1)	^e	M1/E2
669.9	(29/2 ⁻) - 25/2 ⁻	<2	^e	(E2)
671.6	9/2 ⁺ - 7/2 ⁺	<2	0.57 ± 0.17	M1/E2
699.4	13/2 ⁺ -	<2	^e	
700.2	27/2 ⁻ - 23/2 ⁻	13(1)	0.97 ± 0.12	E2
702.9	15/2 ⁺ - 11/2 ⁺	9(1)	1.01 ± 0.15	E2
703.9	19/2 ⁺ - 15/2 ⁺	3(1)	1.08 ± 0.13	E2
704.9	- 13/2 ⁺	<2	^e	
707.2	21/2 ⁺ - 17/2 ⁺	5(1)	1.02 ± 0.19	E2
711.5	13/2 ⁺ - 9/2 ⁺	8(1)	1.00 ± 0.14	E2
753.2	17/2 ⁺ - 13/2 ⁺	10(1)	0.93 ± 0.12	E2
769.7	(31/2 ⁻) - (27/2 ⁻)	2(1)	^e	(E2)
776.3		<2	^e	
783.3	9/2 ⁺ - 7/2 ⁺	3(1)	^e	M1/E2
795.6	11/2 ⁻ - 7/2 ⁺	34(2)	1.20 ± 0.15	M2
800.4	23/2 ⁺ - 19/2 ⁺	2(1)	0.91 ± 0.11	E2
802.6	19/2 ⁻ - 15/2 ⁻	<2	0.93 ± 0.17	E2
810.7	25/2 ⁺ - 21/2 ⁺	3(1)	1.04 ± 0.30	E2
813.0	31/2 ⁻ - 27/2 ⁻	8(1)	1.04 ± 0.14	E2
816.2	15/2 ⁺ - 11/2 ⁺	4(1)	1.02 ± 0.12	E2
820.2	19/2 ⁺ - 15/2 ⁺	4(1)	1.23 ± 0.27	E2
830.5	(33/2 ⁻) - (29/2 ⁻)	<2	^e	(E2)
842.3		<2	^e	
872.2	27/2 ⁺ - 23/2 ⁺	<2	0.99 ± 0.14	E2
876.3	13/2 ⁺ - 9/2 ⁺	4(1)	1.03 ± 0.11	E2
885.0	(35/2 ⁻) - (31/2 ⁻)	<2	^e	(E2)
886.2	29/2 ⁺ - 25/2 ⁺	<2	0.81 ± 0.18	E2
891.4	19/2 ⁻ - 15/2 ⁻	2(1)	^e	E2 [§]
898.0	21/2 ⁺ - 17/2 ⁺	4(1)	^e	E2
902.3	25/2 ⁺ - 21/2 ⁺	2(1)	^e	E2
908.0	(35/2 ⁻) - 31/2 ⁻	3(1)	^e	(E2)
921.9	(31/2 ⁺) - 27/2 ⁺	<2	^e	(E2)
938.6	(35/2 ⁺) - (31/2 ⁺)	<2	^e	(E2)
938.7	(33/2 ⁺) - 29/2 ⁺	<2	^e	(E2)
944.0	23/2 ⁺ - 19/2 ⁺	3(1)	0.86 ± 0.17	E2
945.7	(37/2 ⁻) - (33/2 ⁻)	<2	^e	(E2)
960.3	- 7/2 ⁺	3(1)	^e	
992.1	(39/2 ⁻) - (35/2 ⁻)	<2	^e	(E2)
995.4	(37/2 ⁺) - (33/2 ⁺)	<2	^e	(E2)
1000.2	15/2 ⁻ - 11/2 ⁻	70(4)	1.06 ± 0.13	E2
1009.5	(39/2 ⁻) - (35/2 ⁻)	<2	^e	(E2)
1026.8	(27/2 ⁺) - 23/2 ⁺	<2	^e	(E2)
1032.6	(25/2 ⁺) - 21/2 ⁺	<2	^e	(E2)
1045.0	13/2 ⁺ - 9/2 ⁺	2(1)	0.93 ± 0.20	E2
1067.8	(41/2 ⁺) - (37/2 ⁺)	<2	^e	(E2)
1068.5	(41/2 ⁻) - (37/2 ⁻)	<2	^e	(E2)
1076.5	(43/2 ⁻) - (39/2 ⁻)	<2	^e	(E2)
1089.3	7/2 ⁺ - 5/2 ⁺	14(2)	0.31 ± 0.05	M1/E2
1089.8	15/2 ⁻ - 11/2 ⁻	26(1)	0.93 ± 0.06	E2
1093.5		<2	^e	
1160.2	9/2 ⁺ - 5/2 ⁺	100(7)	1.02 ± 0.04	E2
1182.7	11/2 ⁺ - 7/2 ⁺	7(1)	0.98 ± 0.14	E2
1234.0	9/2 ⁺ - 7/2 ⁺	<2	0.36 ± 0.06	M1/E2
1310.8	9/2 ⁺ - 5/2 ⁺	22(2)	1.23 ± 0.20	E2
1323.1	11/2 ⁻ - 5/2 ⁺	63(3)	1.44 ± 0.15	E3
1512.2	11/2 ⁺ - 7/2 ⁺	<2	^e	E2

^aTransition energies accurate to within ±0.2 keV.

^bIntensities are normalized to 100 for the 1160.2-keV transition.

^cTransition not observed in this experiment, but is reported in Ref. [2].

^dTransition not observed in this experiment, but is reported in Ref. [20].

^eTransition too weak to yield DCO ratio, or the presence of a nearby transition prevents extraction of a DCO ratio.

^fAngular distributions have been measured for these transitions in Ref. [2].

[§]Angular distributions have been measured for these transitions in Ref. [20].

TABLE II. Table giving information on transitions assigned to ^{119}Sb .

Energy, keV ^a	$I_i^\pi - I_f^\pi$	Intensity ^b	DCO ratio	Multipolarity
40.8	$11/2^+ - 11/2^-$	<2 ^c	c, d	<i>E1</i>
134.2	$19/2^- - 17/2^+$	56(2)	0.47 ± 0.04	<i>E1</i>
146.6	$29/2^- - 27/2^-$	<2	0.40 ± 0.13	<i>M1/E2</i>
153.3	$11/2^- - 9/2^+$	43(1)	0.63 ± 0.03	<i>E1</i>
157.4	$11/2^+ -$	<2	d	
164.0	$9/2^+ - 7/2^+$	<2	d	
196.5	$15/2^- - 13/2^-$	<2	d	<i>M1/E2</i>
227.1	$19/2^- - 17/2^-$	7(1)	0.51 ± 0.10	<i>M1/E2</i>
230.9	$19/2^- - 17/2^-$	2(1)	0.74 ± 0.15	<i>M1/E2</i>
232.3	$17/2^- - 15/2^-$	2(1)	0.40 ± 0.10	<i>M1/E2</i>
239.7	$19/2^- - 15/2^-$	11(2)	d	<i>E2</i>
270.4	$7/2^+ - 5/2^+$	105(1)	0.63 ± 0.02	<i>M1/E2</i>
273.1	$15/2^- - 13/2^+$	<2	d	<i>E1</i>
286.1	$21/2^- - 19/2^-$	7(1)	0.74 ± 0.14	<i>M1/E2</i>
288.1	$21/2^- - 19/2^-$	11(2)	0.65 ± 0.17	<i>M1/E2</i>
331.1	$(27/2^+) - 25/2^+$	<2	d	<i>(M1/E2)</i>
334.9	$13/2^+ - 11/2^+$	83(1)	0.85 ± 0.03	<i>M1/E2</i> ^e
357.5	$23/2^- - 21/2^-$	5(1)	0.85 ± 0.16	<i>M1/E2</i>
361.8	$15/2^+ - 13/2^+$	69(1)	0.85 ± 0.03	<i>M1/E2</i> ^e
369.8	$11/2^+ - 9/2^+$	100(1)	0.84 ± 0.03	<i>M1/E2</i> ^e
381.7	$17/2^+ - 15/2^+$	66(1)	0.92 ± 0.04	<i>M1/E2</i> ^e
397.7	$(29/2^+) - (27/2^+)$	<2	d	<i>(M1/E2)</i>
407.0	$25/2^- - 23/2^-$	3(1)	0.91 ± 0.17	<i>M1/E2</i>
413.7	$(31/2^+) - (29/2^+)$	<2	d	<i>(M1/E2)</i>
426.9	$25/2^+ - 23/2^+$	2(1)	0.72 ± 0.21	<i>M1/E2</i>
429.6	$19/2^+ - 17/2^+$	10(1)	0.62 ± 0.08	<i>M1/E2</i>
429.9	$27/2^- - 25/2^-$	2(1)	0.71 ± 0.46	<i>M1/E2</i>
455.8	$(29/2^-) - 27/2^-$	<2	d	<i>(M1/E2)</i>
461.3	$21/2^+ - 19/2^+$	7(1)	0.61 ± 0.10	<i>M1/E2</i>
474.2	$23/2^+ - 21/2^+$	4(1)	0.61 ± 0.13	<i>M1/E2</i>
479.9	$(31/2^-) - (29/2^-)$	<2	d	<i>(M1/E2)</i>
489.8	$25/2^+ - 23/2^+$	2(1)	0.95 ± 0.28	<i>M1/E2</i>
497.3	$19/2^- - 15/2^-$	9(1)	0.96 ± 0.09	<i>E2</i>
510.9	$(27/2^+) - 25/2^+$	2(1)	d	<i>(M1/E2)</i>
605.9	$23/2^- - 19/2^-$	8(1)	0.98 ± 0.12	<i>E2</i>
630.7	$(17/2^+) - 13/2^+$	3(1)	d	<i>(E2)</i>
643.7	$23/2^- - 19/2^-$	<2	d	<i>E2</i>
653.3	$(15/2^+) - (11/2^+)$	<2	d	<i>E2</i>
689.7	$27/2^- - 23/2^-$	3(1)	0.90 ± 0.19	<i>E2</i>
696.9	$15/2^+ - 11/2^+$	15(1)	0.97 ± 0.10	<i>E2</i>
700.3	$9/2^+ - 7/2^+$	82(1)	0.57 ± 0.03	<i>M1/E2</i>
704.9	$13/2^+ - 9/2^+$	15(1)	0.94 ± 0.10	<i>E2</i>
730.3	$(11/2^+) - 11/2^-$	<2	d	<i>E1</i>
731.0	$13/2^+ - 11/2^+$	<2	0.53 ± 0.25	<i>M1/E2</i>
736.4	$(21/2^+) - (17/2^+)$	2(1)	d	<i>(E2)</i>
743.7	$17/2^+ - 13/2^+$	19(1)	1.08 ± 0.21	<i>E2</i>
744.2	$27/2^- - 23/2^-$	3(1)	0.90 ± 0.17	<i>E2</i>
750.8	$17/2^- - 15/2^-$	2(1)	0.31 ± 0.10	<i>M1/E2</i>
754.7	$17/2^- - 15/2^-$	2(1)	0.26 ± 0.11	<i>M1/E2</i>
764.8	$25/2^- - 21/2^-$	<2	d	<i>E2</i>
794.8	$13/2^+ - 11/2^+$	<2	d	<i>M1/E2</i>
811.4	$19/2^+ - 15/2^+$	4(1)	d	<i>E2</i>
836.2	$27/2^- - 23/2^-$	<2	d	<i>E2</i>
836.5	$(25/2^+) - (21/2^+)$	<2	d	<i>(E2)</i>
837.8	$(31/2^-) - 27/2^-$	2(1)	d	<i>(E2)</i>

TABLE II. (Continued).

Energy, keV ^a	$I_i^\pi - I_f^\pi$	Intensity ^b	DCO ratio	Multipolarity
876.5	$19/2^- - 17/2^+$	2(1)	0.65 ± 0.20	$E1$
881.6	$(11/2^+) - 9/2^+$	<2	^d	
885.7	$(29/2^-) - 25/2^-$	<2	^d	($E2$)
888.6	$13/2^+ -$	<2	^d	
891.0	$21/2^+ - 17/2^+$	2(1)	^d	$E2$
901.5	$(29/2^+) - (25/2^+)$	<2	^d	($E2$)
912.5	$13/2^- - 11/2^-$	4(1)	0.45 ± 0.19	$M1/E2$
923.4	$(35/2^-) - (31/2^-)$	<2	^d	($E2$)
925.7	$13/2^+ - 9/2^+$	2(1)	0.89 ± 0.25	$E2$
935.7	$23/2^+ - 19/2^+$	2(1)	^d	$E2$
935.8	$(31/2^-) - 27/2^-$	<2	^d	($E2$)
942.2	$9/2^+ - 7/2^+$	3(1)	0.43 ± 0.13	$M1/E2$
947.8	$15/2^- - 11/2^-$	22(1)	1.01 ± 0.08	$E2$
963.8	$25/2^+ - 21/2^+$	<2	^d	$E2$
970.8	$9/2^+ - 5/2^+$	36(1)	0.99 ± 0.08	$E2$
979.2	$-7/2^+$	5(1)	^d	
989.8	$13/2^+ - 9/2^+$	2(1)	0.95 ± 0.18	$E2$
1031.0	$17/2^- - 15/2^+$	4(1)	0.49 ± 0.14	$E1$
1046.0	$(11/2^+) - (7/2^+)$	<2	^d	$E2$
1048.3	$(7/2^+) - 5/2^+$	2(1)	^d	$E2$
1095.6	$11/2^- - 7/2^+$	<2	^d	$M2$
1109.1	$15/2^- - 11/2^-$	5(1)	0.90 ± 0.16	$E2$
1136.7	$11/2^+ - 7/2^+$	11(1)	0.97 ± 0.10	$E2$
1138.9	$15/2^- - 11/2^-$	9(1)	1.05 ± 0.19	$E2$
1212.6	$9/2^+ - 5/2^+$	33(1)	1.02 ± 0.08	$E2$

^aTransition energies accurate to within ± 0.2 keV.

^bIntensities are normalized to 100 for the 369.8-keV transition.

^cTransition not observed, but inferred from γ -coincidence relations.

^dTransition too weak to yield DCO ratio, or the presence of a nearby transition prevents extraction of a DCO ratio.

^eAngular distributions have been measured for these transitions in Ref. [2].

DCO ratios. Thus, under this presumption this sequence extends to $J^\pi = (31/2^+)$.

A second strongly coupled band has also been observed in this experiment. This structure was found to be populated to 4%. This band, which is labeled band 4 in Fig. 1 begins at $J^\pi = 19/2^-$ and extends to $J^\pi = (31/2^-)$. The spins of this band are rather well established from the DCO ratios of the transitions depopulating the band to the lower spin levels. The state at 2314 keV, depopulated by the 948-keV γ ray, has a spin of $15/2^-$; this has been established in Ref. [2] through angular distribution measurements. The DCO ratios for the 231-, 227-, 751-, 755-, 877-, and 1031-keV transitions which depopulate this band then strongly imply the spin of the bottom member of band 4 to be $19/2$. The DCO ratios are not able to rule out a positive parity for this band. It has been assigned negative parity in this work based on a comparison with ^{117}Sb .

Two, and possibly three, decoupled bands were also observed in this study. Band 2 is a sequence of transitions extending from $J^\pi = 13/2^+$ to $J^\pi = (29/2^+)$. This band was populated with only 1% of the ^{119}Sb channel strength; as a result of the low intensity it was only possible to obtain a DCO ratio for the first transition in the sequence. However, the energies of these transitions and a comparison with the

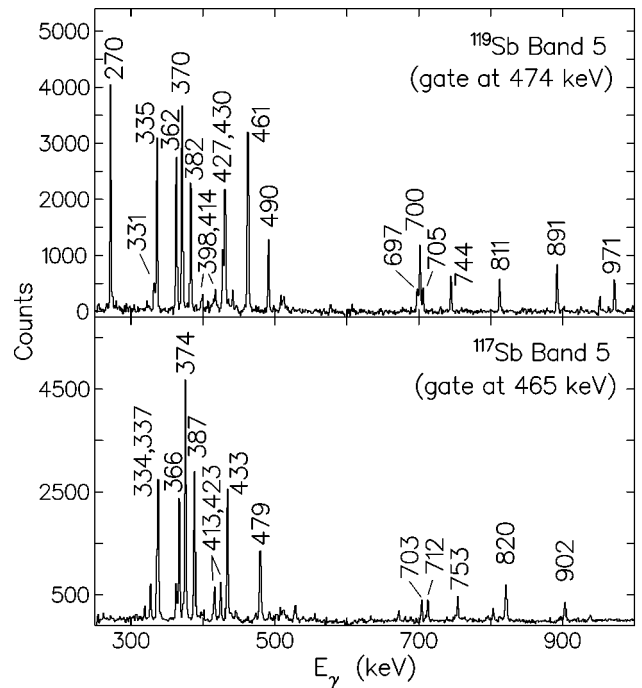


FIG. 2. Two background subtracted coincidence spectra showing the $\pi(d_{5/2, 7/2}^2 \otimes (\pi g_{9/2})^{-1})$ bands in $^{117,119}\text{Sb}$.

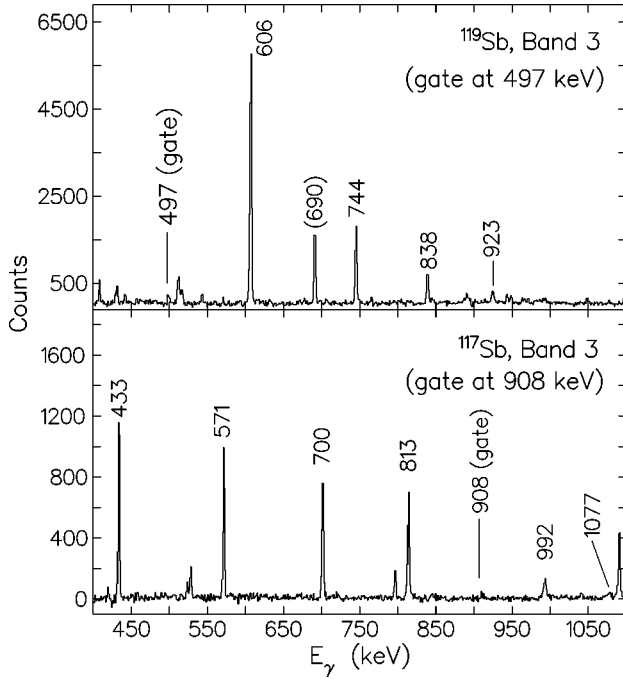


FIG. 3. Two background subtracted coincidence spectra showing the $\pi h_{11/2}(d_{5/2}g_{7/2})^2 \otimes (\pi g_{9/2})^{-2}$ bands in $^{117,119}\text{Sb}$.

level scheme of ^{117}Sb suggest $E2$ assignments for these two upper band members. The spin and parity of the $13/2^+$ state are well established through the DCO ratios of the transitions depopulating the band. The positive-parity assignment is also supported by the fact that this band decays only weakly into known negative-parity states. The link to the negative-parity states is accomplished via a 41-keV transition which was not directly observed in this experiment. Its presence was inferred from coincidence relationships between band 2 and the 153-keV transition.

Band 3 is a decoupled band extending from $J^\pi=15/2^-$ to $J^\pi=(35/2^-)$, populated with approximately 4% of the reaction channel cross section. DCO ratios imply that all but the final two transitions in this cascade have $E2$ character; it was not possible to extract a DCO ratio for the uppermost transitions. The 1139-keV γ -ray transition depopulating this band was found to have a DCO ratio of 1.05 ± 0.19 which thus determines the spins and parities of the band as shown in Fig. 1. The band decays exclusively into the $11/2^-$ state. A spectrum representing this band can be seen in Fig. 3.

Finally, another structure observed has been labeled band 1 in Fig. 1. This structure consists of only one in-band transition, with four transitions depopulating it. The intensity flows mainly through a strong $J^\pi=7/2^+ - 5/2^+$ transition. DCO ratios were unavailable for all of the five transitions involved in this structure. It has been singled out for attention here due to the similarity between it and band 1 in ^{117}Sb .

IV. DISCUSSION

A. Spherical levels in ^{117}Sb and ^{119}Sb

At lower spins, the shapes of the $_{51}\text{Sb}$ nuclei are dominated by the major shell gap at $Z=50$. With only one proton outside the closed shell, the Sb nuclei are expected to behave

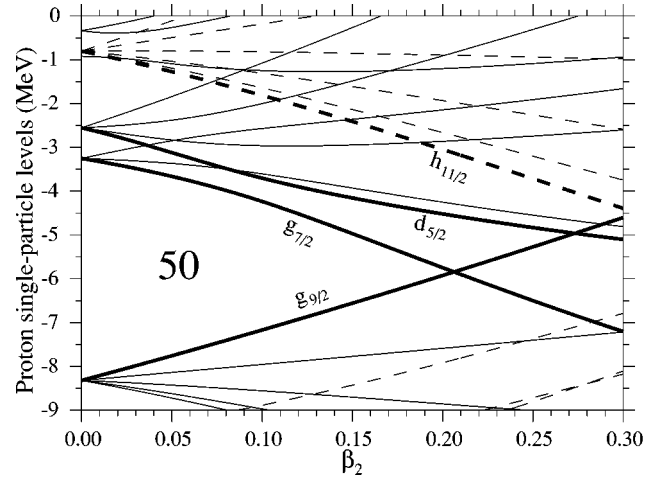


FIG. 4. Woods-Saxon energy levels as a function of the deformation parameter β_2 . The $Z=50$ energy gap and some orbitals are labeled.

like spherical shell-model nuclei with the valence proton occupying the $d_{5/2}$, $g_{7/2}$, and $h_{11/2}$ orbitals. A Woods-Saxon level diagram for the proton orbitals is shown in Fig. 4 with $\beta_2=0$ representing a spherical nucleus. The neutrons outside of $N=50$ occupy a similar shell-model space with the Fermi level depending on the neutron number N . Although the low-spin levels are numerous, they can often be described in terms of a simple coupling of the valence proton orbitals to various spherical states of the $_{50}\text{Sn}$ core, as is the case for $^{117,119}\text{Sb}$. The ground states of these two nuclei have $J^\pi=5/2^+$, which results from the occupation of the $\pi d_{5/2}$ orbital coupled to the ground state of the corresponding $_{50}\text{Sn}$ core nucleus. The level schemes of these two nuclei also show low-lying $7/2^+$ and $11/2^-$ states from the occupation of the $\pi g_{7/2}$ and $\pi h_{11/2}$ orbitals, respectively.

The even-mass Sn nuclei all possess $0^+ - 2^+ - 4^+$ ground-state sequences of similar high energies, and negative-parity spherical levels which result from the breaking of a neutron pair to include an odd number of $h_{11/2}$ orbitals. The coupling of the valence proton to these states can be seen in both ^{117}Sb and ^{119}Sb . For example, these nuclei exhibit prominent $9/2^+$, $11/2^+$, and $15/2^-$ spherical levels, which can be attributed to $(j \otimes 2^+)$, namely the coupling of the spherical 2^+ state of the core to the $\pi d_{5/2}$, $\pi g_{7/2}$ and $\pi h_{11/2}$ orbitals, respectively. A good example of the valence proton coupling to a negative parity core state is the $19/2^-$ isomer in ^{119}Sb . It has been shown in previous studies that this state is composed of the $\pi d_{5/2}$ orbital coupled to the two-neutron 7^- state of the ^{118}Sn core [22]. The negative parity 202-254-292 sequence in ^{117}Sb and 273-232 sequence in ^{119}Sb can also be explained via a similar coupling picture [23,24].

B. Positive parity strongly coupled bands

A single strongly coupled band having positive parity was observed in both ^{117}Sb and ^{119}Sb . The experimental Routhians [25] for these two bands are shown in Fig. 5, when a Harris parametrization $\mathcal{J}_0=17$ and $\mathcal{J}_1=12$ has been employed [5]; as can be seen, the bands have zero signature splitting. These strongly coupled bands in the odd-Sb isotopes have been systematically studied in previous investiga-

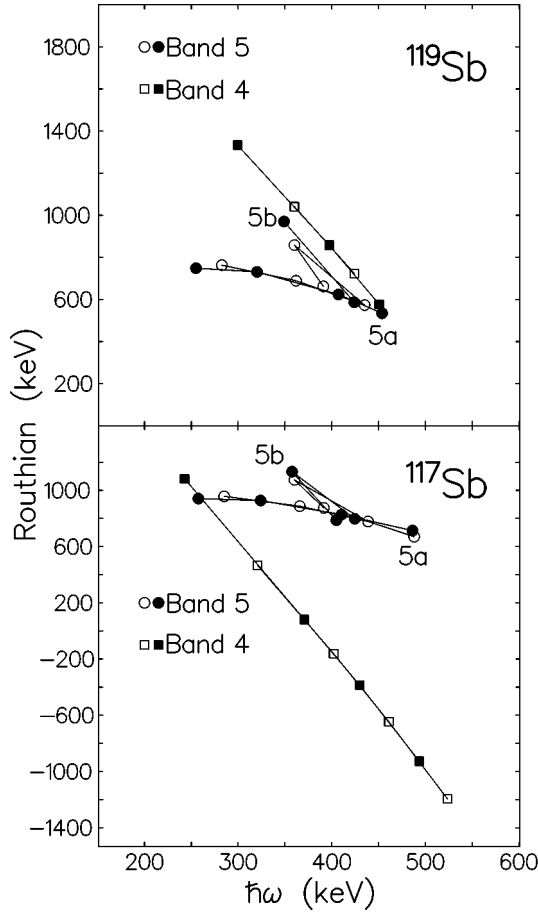


FIG. 5. Experimental Routhians extracted from the strongly coupled bands uncovered in this study. The top frame shows the Routhians from ^{119}Sb , the bottom those from ^{117}Sb . In both frames, filled data points indicate the favored signature, and open points the unfavored signature. The Harris parameters $\mathcal{T}_0=17$ and $\mathcal{T}_1=12$ were used in the calculations.

tions [1,2]. Modest deformations arise via 1p-1h proton excitations across the $Z=50$ gap because of a hole in the upsloping $\pi g_{9/2}$ orbital and two protons in the downsloping $\pi g_{7/2}$ orbital (see Fig. 4). These bands are thus based on a 2p-1h proton configuration, given as $(\pi g_{7/2}d_{5/2})^2 \otimes (\pi g_{9/2})^{-1}$. The high K of the $(\pi g_{9/2})^{-1}$ orbital is responsible for the lack of signature splitting.

Although these bands in $^{117,119}\text{Sb}$ have each been extended several transitions, it is the sequences labeled band 5b in Fig. 1 which represent an added interest to these structures. These are short sequences of presumably dipole character, which feed into bands 5a of $^{117,119}\text{Sb}$ at the $21/2^+$ and $23/2^+$ states. The Routhians for these short sequences are shown along with the Routhians for the $(\pi g_{7/2})^2 \otimes (\pi g_{9/2})^{-1}$ bands. It can be seen that band 5b crosses band 5a at a rotational frequency $\hbar\omega \approx 0.4$ MeV. Since this feature is reminiscent of a quasiparticle alignment, the relative alignments [25] of bands 5a and 5b have been calculated, using the same Harris parameters as employed in the calculation of the Routhians. The relative alignments are shown in Fig. 6. The bands 5b in both ^{117}Sb and ^{119}Sb gain approximately $7\hbar$ in alignment as a result of this crossing.

This crossing can be explained as an $h_{11/2}$ neutron crossing. Such crossings in $(\pi g_{9/2})^{-1}$ bands have been observed

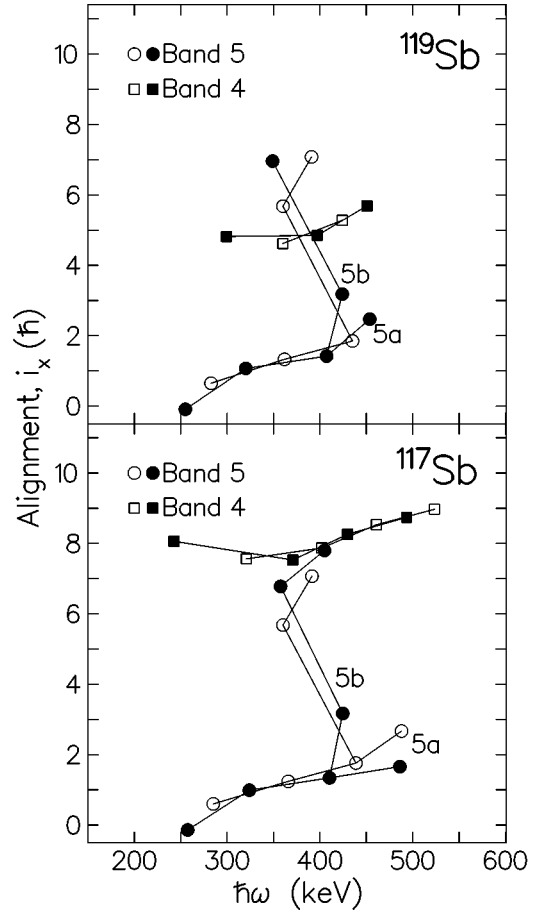


FIG. 6. Experimental relative alignments extracted from the strongly coupled bands uncovered in this study. The top frame shows the alignments from ^{119}Sb , the bottom those from ^{117}Sb . In both frames, filled data points indicate the favored signature, and open points the unfavored signature. The Harris parameters $\mathcal{T}_0=17$ and $\mathcal{T}_1=12$ were used in the calculations.

previously in $Z=53$ and 55 isotopes, and should be expected to occur in $^{117,119}\text{Sb}$. Cranked shell model (CSM) calculations [26] performed for ^{117}Sb are shown in Fig. 7. An axial deformation $\beta_2=0.22$ has been used [9]. These calculations predict this crossing to occur at a rotational frequency $\hbar\omega \approx 0.35$ MeV, slightly lower than the experimental value, but in reasonable agreement with experiment. The $\nu h_{11/2}$ alignment also explains the large gain in the relative alignment of the bands. Another crossing which is expected to occur at a nearby frequency, namely the $\pi g_{7/2}$ crossing, cannot explain such a large alignment increase.

C. Negative-parity strongly coupled bands

In each of the two nuclei under study, a single negative-parity strongly coupled band was observed. These are shown as bands 4 in Fig. 1. The two bands are similar in that both have zero signature splitting, as can be seen in Fig. 5, where the experimental Routhians of the bands are plotted. The relative alignments of these bands are shown in Fig. 6. In calculating the experimental Routhians and alignments, a Harris parametrization $\mathcal{J}_0=17$ and $\mathcal{J}_1=12$ was employed [5]. Neither band shows evidence of a quasiparticle alignment, even though the bands were observed to rotational

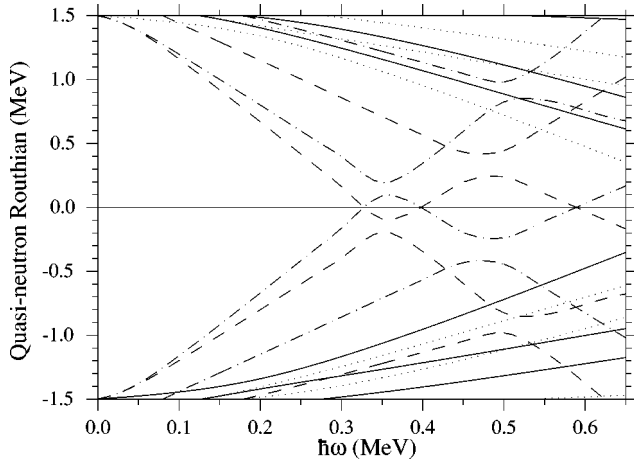


FIG. 7. Cranked shell-model calculations performed for neutrons in ^{117}Sb . An axial deformation of $\beta_2=0.22$ was used in the calculations. Solid lines indicate orbitals having both positive parity and signature; dotted lines, positive parity and negative signature; dashed lines, negative parity and signature; and dash-dotted lines, negative parity and positive signature.

frequencies near or above the frequency at which the $\nu h_{11/2}$ alignment was observed in the $(\pi g_{7/2}d_{5/2})^2 \otimes (\pi g_{9/2})^{-1}$ bands. These two bands differ in one important aspect; the bandhead of band 4 in ^{119}Sb was observed $2\hbar$ lower than that of band 4 in ^{117}Sb .

Previous studies of ^{117}Sb provide the quasiparticle configurations for these two structures. Band 4 in ^{117}Sb is built upon a $23/2^-$ isomer, which has been extensively studied in Refs. [21,20]. In these prior studies it was shown that the $23/2^-$ isomer possesses a significant deformation [21], and a g factor consistent with a $[(\pi g_{7/2}d_{5/2})^2 \otimes (\pi g_{9/2})^{-1}] \otimes \nu 7^-$ quasiparticle configuration [20]. Here the $\nu 7^-$ refers to a spherical state of the ^{116}Sn core, having a $\nu h_{11/2}d_{3/2}$ configuration. This configuration, which is assigned to band 4 in ^{117}Sb in the present study, is consistent with the lack of signature splitting in this band, due to the high K of the $(\pi g_{9/2})^{-1}$ orbital. The lack of the AB $\nu h_{11/2}$ alignment is then also understood, since this two-neutron configuration blocks this crossing. One can also see in Fig. 6 that the BC $\nu h_{11/2}$ alignment is not present in this band, although the CSM calculations of Fig. 7 predict this crossing to occur at $\hbar\omega \approx 0.50$ MeV. Since the AB $\nu h_{11/2}$ crossing is delayed in the positive-parity coupled bands, it may not be unreasonable to expect a similar delay in this case. It is worth noting, however, that the experimentally deduced deformation for band 4 in ^{117}Sb is $\beta_2=0.24$ [21], while the calculation shown in Fig. 7 was performed for $\beta_2=0.22$. If the calculation is performed instead with $\beta_2=0.24$, the BC crossing is predicted to increase to $\hbar\omega \approx 0.52$ MeV, close to the highest observed frequency of the band.

Band 4 in ^{119}Sb results from a similar configuration. In order to explain the lower spin of this band compared to band 4 in ^{117}Sb , there are two options both involving the $(\pi g_{7/2}d_{5/2})^2 \otimes (\pi g_{9/2})^{-1}$ proton configuration, which is required to account for the lack of signature splitting in this structure. The first involves a coupling of this proton configuration to the known two-neutron 5^- state of the ^{118}Sn core. This $\nu 5^-$ spherical state involves a single $h_{11/2}$ neutron,

which again explains the nonobservation of the $\nu h_{11/2}$ alignment. The second option, as in ^{117}Sb , simply involves a coupling of the proton configuration to the $\nu 7^-$ ^{118}Sn core state; however, in this case the coupling would not be fully aligned.

D. Decoupled bands

1. Configurations

A total of five decoupled rotational bands were observed in these experiments. The three found in ^{117}Sb have been discussed in Ref. [4], where they were explained as a coupling of a low- K valence proton to the 2p-2h deformed structure known in the ^{116}Sn core. Thus, the configurations of these bands were determined to be $\pi g_{7/2} \otimes 2p2h$, $\pi d_{5/2} \otimes 2p2h$, $\pi h_{11/2} \otimes 2p2h$, where 2p2h represents the proton two-particle-two-hole structure $(\pi g_{7/2}d_{5/2})^2 \otimes (\pi g_{9/2})^{-2}$ responsible for the band in ^{116}Sn . Because of the near degeneracy of the $\pi g_{7/2}$ and the $\pi d_{5/2}$ orbitals, the two positive-parity protons, $(\pi g_{7/2}d_{5/2})^2$, in the 2p-2h configuration may change somewhat depending on the valence proton. These assignments are supported by the observed spins of the bands, and by the observed decay patterns to the lower-lying spherical single-particle states. On the basis of the spins, the three decoupled bands in the ^{117}Sb begin to branch out at the levels corresponding to the ^{116}Sn 4^+ 2p-2h band member, decaying respectively to both the spherical and the deformed ($j \otimes 2^+$) states, which are admixed. Thus, the $19/2^-$ member of the $\pi h_{11/2}$ band 3 decays into two $15/2^-$ states, the $13/2^+$ member of the $\pi d_{5/2}$ band 2 decays into two $9/2^+$ states, and the $15/2^+$ member of the $\pi g_{7/2}$ band 1 decays into two $11/2^+$ states.

Using this information, it is possible to assign configurations to the decoupled bands in ^{119}Sb . Band 3, having negative parity and decaying exclusively into the spherical $11/2^-$ state, can be assigned the $\pi h_{11/2} \otimes 2p2h$ configuration. Although the relationship between the decay pattern and the orbital occupied by the valence proton is not as clear as in ^{117}Sb , the spins of band 2 are indicative of the $\pi d_{5/2} \otimes 2p2h$ configuration. Finally, band 1 is possibly related to the $\pi g_{7/2} \otimes 2p2h$ configuration; this must be considered tentative, however, as the spins and parity of this structure are unknown.

Band 1a in ^{117}Sb remains to be explained. This sequence was only weakly populated, thus only the lowest state of the sequence is known with any certainty. However, this sequence does exhibit bandlike energy spacings. Presuming the three transitions of this structure are of stretched $E2$ character, this sequence may be the signature partner to band 1 with the expected large signature splitting.

The observation of decoupled bands involving 2p-2h excitations across the $Z=50$ gap in $_{50}\text{Sn}$ and $_{51}\text{Sb}$ nuclei has also been extended to $_{52}\text{Te}$ [27,28] and $_{53}\text{I}$ [29–32].

2. Quasiparticle alignments in the decoupled bands

The $\nu h_{11/2}$ pair alignment which was observed in the $(\pi g_{7/2}d_{5/2})^2 \otimes (\pi g_{9/2})^{-1}$ strongly coupled bands should be seen in the decoupled bands as well. Such alignments can be seen in the dynamic moments of inertia $\mathcal{J}^{(2)}$ of the positive parity bands, which are shown in Fig. 8. Bands 1 and 2 in

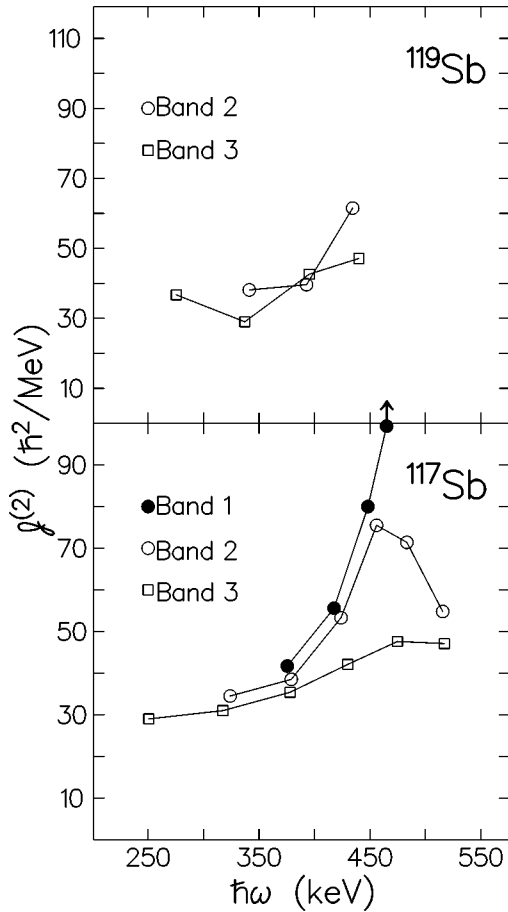


FIG. 8. Plot of the dynamic moment of inertia ($\mathcal{J}^{(2)}$) extracted from the decoupled bands observed in these experiments for ^{119}Sb (top) and ^{117}Sb (bottom).

^{117}Sb clearly show an alignment at $\hbar\omega \approx 0.45$ MeV, and band 2 in ^{119}Sb at least shows a strong increase in $\mathcal{J}^{(2)}$. The negative-parity bands also show evidence of this crossing. In both nuclei, the dynamic moment of inertia of bands 3 show a gradual increase, and in ^{117}Sb the $\mathcal{J}^{(2)}$ appears to have begun to decrease at the last point.

Although the expected $\nu h_{11/2}$ alignments are observed, the frequencies at which they occur are not well reproduced by the CSM calculations. The calculations shown in Fig. 7 for a deformation of $\beta_2 = 0.22$ predict this crossing to occur at $\hbar\omega \approx 0.35$ MeV, considerably lower than the observed values; a higher deformation value of $\beta_2 = 0.30$ is required to achieve the observed crossing frequency of 0.45 MeV. Although this value is considerably larger than the $\beta_2 = 0.22$ for the $(\pi g_{7/2} d_{5/2})^2 \otimes (\pi g_{9/2})^{-1}$ bands, it may not be unreasonable. The decoupled bands involve a 2p-2h excitation across the gap while the strongly coupled bands involve only a 1p-1h excitation. Thus there is an additional hole in the up-sloping $\pi g_{9/2}$ orbital and an additional proton in a low- K down-sloping orbital, both of which achieve further β -driving forces. Furthermore, the deformation of the $\pi h_{11/2} \otimes 2p2h$ band known in ^{113}Sb has been measured through the extraction of the average transition quadrupole moment of the band, yielding a value of $\beta = 0.3$ [5].

Finally, there is the matter of the interaction strengths of the $\nu h_{11/2}$ pair alignments. The $\mathcal{J}^{(2)}$ for the three decoupled bands in ^{117}Sb clearly show a difference in the interaction

strengths between the positive- and negative-parity bands. This is evidenced from the sharpness of the peak in the $\mathcal{J}^{(2)}$ of the positive-parity bands, and the comparatively gradual increase in the $\pi h_{11/2}$ band. The gradual increase associated with the alignment implies a stronger interaction strength. The fact that the interaction strength is different for bands in the same nucleus cannot be explained by standard CSM calculations such as that shown in Fig. 7; however, this effect has been observed previously, and attributed to a residual proton-neutron interaction which is not included in the standard cranked shell model [5,9,33]. The stronger p - n interaction arises since the aligning neutrons and the valence proton occupy similar $h_{11/2}$ orbitals, and thus the overlap of their wave functions is maximized.

V. CONCLUSIONS

High-spin states have been identified in ^{117}Sb and ^{119}Sb . The previously known $(\pi g_{7/2} d_{5/2})^2 \otimes (\pi g_{9/2})^{-1}$ bands involving 1p-1h proton excitations across the $Z=50$ gap have been extended to higher spin, and an alignment of a $\nu h_{11/2}$ neutron pair identified. A negative-parity strongly coupled band was found in each nucleus as well, resulting from a coupling of the $(\pi g_{7/2})^2 \otimes (\pi g_{9/2})^{-1}$ structure to the 5^- and 7^- spherical two-neutron states of the $^{116,118}\text{Sn}$ core nuclei, respectively.

A number of decoupled bands, which involve 2p-2h proton excitations across the gap, were discovered in ^{117}Sb and in ^{119}Sb . These bands represent a coupling of the valence proton to deformed $(\pi g_{7/2} d_{5/2})^2 \otimes (\pi g_{9/2})^{-2}$ states of the $^{116,118}\text{Sn}$ cores. The ^{117}Sb nucleus proved to be the best illustration of these structures, as three decoupled bands were observed, and each conclusively linked to the occupation of the three available valence proton orbitals, $d_{5/2}$, $g_{7/2}$, and $h_{11/2}$, above $Z=50$. The expected $\nu h_{11/2}$ pair alignment was observed in these bands, although at a higher frequency than expected by the cranked shell model, suggesting a larger deformation. The alignment of the $h_{11/2}$ neutrons in the $\pi h_{11/2}$ band was found to differ from that of the $\pi g_{7/2}$ and $\pi d_{5/2}$ bands, in a manner consistent with a residual proton-neutron interaction, as has been previously reported [5,9,33]. Of course there may be other considerations, notably quadrupole pairing as discussed in Ref. [34].

Finally, a large number of new single-particle states was found. These states show the irregular energies typical of shell-model nuclei. Many can be explained by simple coupling of the valence proton orbitals to known spherical states in the $^{116,118}\text{Sn}$ core nuclei. Thus the $^{117,119}\text{Sb}$ nuclei have been observed to possess a wide range of both spherical and deformed states, all of which relate to a coupling of the valence proton to the different structures in the $^{116,118}\text{Sn}$ core nuclei.

ACKNOWLEDGMENTS

This work was supported in part by the National Science Foundation. We wish to thank the staff of the Stony Brook facility for the beams and targets. One of us (J.-y.Z.) would like to acknowledge NSF Grant No. INT-9001476.

- [1] A. K. Gaigalas, R. E. Shroy, G. Schatz, and D. B. Fossan, *Phys. Rev. Lett.* **35**, 555 (1975).
- [2] R. E. Shroy, A. K. Gaigalas, G. Schatz, and D. B. Fossan, *Phys. Rev. C* **19**, 1324 (1979); A. K. Gaigalas, R. E. Shroy, G. Schatz, and D. B. Fossan, *Phys. Rev. Lett.* **35**, 55 (1975).
- [3] J. Bron, W. H. A. Hesselink, A. Van Poelgeest, J. J. A. Zalmstra, M. J. Uitzinger, and H. Verheul, *Nucl. Phys.* **A318**, 335 (1979).
- [4] D. R. LaFosse, D. B. Fossan, J. R. Hughes, Y. Liang, P. Vaska, M. P. Waring, and J.-y. Zhang, *Phys. Rev. Lett.* **69**, 1332 (1992).
- [5] V. P. Janzen, H. R. Andrews, B. Haas, D. C. Radford, D. Ward, A. Omar, D. Prévost, M. Sawicki, P. Unrau, J. C. Waddington, T. E. Drake, A. Galindo-Uribarri, and R. Wyss, *Phys. Rev. Lett.* **70**, 1065 (1993).
- [6] V. P. Janzen, D. R. LaFosse, H. Schnare, D. B. Fossan, A. Galindo-Uribarri, J. R. Hughes, S. M. Mullins, E. S. Paul, L. Persson, S. Pilotte, D. C. Radford, I. Ragnarsson, P. Vaska, J. C. Waddington, R. Wadsworth, D. Ward, J. Wilson, and R. Wyss, *Phys. Rev. Lett.* **72**, 1160 (1994).
- [7] H. Schnare, D. R. LaFosse, D. B. Fossan, J. R. Hughes, P. Vaska, K. Hauschild, I. M. Hibbert, R. Wadsworth, V. P. Janzen, D. C. Radford, S. M. Mullins, C. W. Beausang, E. S. Paul, J. DeGraaf, A. V. Afanasjev, and I. Ragnarsson, *Phys. Rev. C* **54**, 1598 (1996).
- [8] G. J. Lane, D. B. Fossan, I. Thorslund, P. Vaska, R. G. Allat, E. S. Paul, L. Käubler, H. Schnare, I. M. Hibbert, N. O'Brien, R. Wadsworth, W. Andrejtscheff, J. de Graaf, J. Simpson, I. Y. Lee, A. O. Macchiavelli, D. J. Blumenthal, C. N. Davids, C. J. Lister, D. Seweryniak, A. V. Afanasjev, and I. Ragnarsson, *Phys. Rev. C* **55**, R2127 (1997).
- [9] D. R. LaFosse, D. B. Fossan, J. R. Hughes, Y. Liang, H. Schnare, P. Vaska, M. P. Waring, J.-y. Zhang, R. M. Clark, R. Wadsworth, S. A. Forbes, E. S. Paul, V. P. Janzen, A. Galindo-Uribarri, D. C. Radford, D. Ward, S. M. Mullins, D. Prévost, and G. Zwartz, *Phys. Rev. C* **50**, 1819 (1994).
- [10] D. R. LaFosse, D. B. Fossan, J. M. Sears, I. Thorslund, P. Vaska, K. Hauschild, I. M. Hibbert, R. Wadsworth, E. S. Paul, S. Mullins, A. V. Afanasjev, and I. Ragnarsson, unpublished.
- [11] R. Wadsworth, H. R. Andrews, R. M. Clark, D. B. Fossan, A. Galindo-Uribarri, J. R. Hughes, V. P. Janzen, D. R. LaFosse, S. M. Mullins, E. S. Paul, D. C. Radford, H. Schnare, P. Vaska, D. Ward, J. N. Wilson, and R. Wyss, *Nucl. Phys.* **A559**, 461 (1993).
- [12] R. Wadsworth, C. W. Beausang, M. Cromaz, J. DeGraaf, D. B. Fossan, S. Flibotte, A. Galindo-Uribarri, K. Hauschild, I. M. Hibbert, G. Hackman, J. R. Hughes, V. P. Janzen, D. R. LaFosse, S. M. Mullins, E. S. Paul, D. C. Radford, H. Schnare, P. Vaska, D. Ward, J. N. Wilson, and I. Ragnarsson, *Phys. Rev. C* **53**, 2763 (1996).
- [13] R. Wadsworth, H. R. Andrews, C. W. Beausang, R. M. Clark, J. DeGraaf, D. B. Fossan, A. Galindo-Uribarri, I. M. Hibbert, K. Hauschild, J. R. Hughes, V. P. Janzen, D. R. LaFosse, S. M. Mullins, E. S. Paul, L. Persson, S. Pilotte, D. C. Radford, H. Schnare, P. Vaska, D. Ward, J. N. Wilson, and I. Ragnarsson, *Phys. Rev. C* **50**, 483 (1994).
- [14] I. Ragnarsson, V. P. Janzen, D. B. Fossan, N. C. Schmeing, and R. Wadsworth, *Phys. Rev. Lett.* **74**, 3935 (1995).
- [15] A. V. Afanasjev and I. Ragnarsson, *Nucl. Phys.* **A591**, 387 (1995).
- [16] R. S. Chakravarthy and R. G. Pillay, *Phys. Rev. C* **54**, 2319 (1996).
- [17] D. R. LaFosse, D. B. Fossan, J. R. Hughes, Y. Liang, H. Schnare, P. Vaska, M. P. Waring, and J.-y. Zhang, unpublished.
- [18] K. S. Krane, R. M. Steffen, and R. M. Wheeler, *Nucl. Data Tables* **11**, 351 (1973).
- [19] D. C. Radford, *Nucl. Instrum. Methods Phys. Res. A* **361**, 297 (1995).
- [20] M. Ionescu-Bujor, A. Iordachescu, G. Pascovici, and C. Stan-Sion, *Nucl. Phys.* **A466**, 317 (1987).
- [21] M. Ionescu-Bujor, A. Iordachescu, G. Pascovici, and V. Sabaïduc, *Phys. Lett. B* **200**, 259 (1988).
- [22] M. Ionescu-Bujor, A. Iordachescu, and G. Pascovici, *Nucl. Phys.* **A531**, 112 (1991).
- [23] S. Lunardi, P. J. Daly, F. Soramel, C. Signorini, B. Fornal, G. Fortuna, A. M. Stefanini, R. Broda, W. Meczynski, and J. Blomqvist, *Z. Phys. A* **328**, 487 (1987).
- [24] L. K. Kostov, W. Andrejtscheff, L. G. Kostova, A. Dewald, G. Böhm, K. O. Zell, P. von Brentano, H. Prade, J. Döring, and R. Schwengner, *Z. Phys. A* **337**, 407 (1990).
- [25] R. Bengtsson and S. Frauendorf, *Nucl. Phys.* **A327**, 139 (1979).
- [26] R. Wyss, private communication.
- [27] E. S. Paul, C. W. Beausang, S. A. Forbes, S. J. Gale, A. N. James, P. M. Jones, M. J. Joyce, H. R. Andrews, V. P. Janzen, D. C. Radford, D. Ward, R. M. Clark, K. Hauschild, I. M. Hibbert, R. Wadsworth, R. A. Cunningham, J. Simpson, T. Davinson, R. D. Page, P. J. Sellin, P. J. Woods, D. B. Fossan, D. R. LaFosse, H. Schnare, M. P. Waring, A. Gizon, J. Gizon, T. E. Drake, J. DeGraaf, and S. Pilotte, *Phys. Rev. C* **50**, 698 (1994).
- [28] I. Thorslund, D. B. Fossan, D. R. LaFosse, H. Schnare, K. Hauschild, I. M. Hibbert, S. M. Mullins, E. S. Paul, I. Ragnarsson, J. M. Sears, P. Vaska, and R. Wadsworth, *Phys. Rev. C* **52**, R2839 (1995).
- [29] E. S. Paul, C. W. Beausang, S. A. Forbes, S. J. Gale, A. N. James, R. M. Clark, K. Hauschild, I. M. Hibbert, R. Wadsworth, R. A. Cunningham, J. Simpson, T. Davinson, R. D. Page, P. J. Sellin, P. J. Woods, D. B. Fossan, D. R. LaFosse, H. Schnare, M. P. Waring, A. Gizon, and J. Gizon, *Phys. Rev. C* **48**, R490 (1993).
- [30] M. P. Waring, E. S. Paul, C. W. Beausang, R. M. Clark, R. A. Cunningham, T. Davinson, S. A. Forbes, D. B. Fossan, S. J. Gale, A. Gizon, J. Gizon, K. Hauschild, I. M. Hibbert, A. N. James, P. M. Jones, M. J. Joyce, D. R. LaFosse, R. D. Page, I. Ragnarsson, H. Schnare, P. J. Sellin, J. Simpson, P. Vaska, R. Wadsworth, and P. J. Woods, *Phys. Rev. C* **51**, 2427 (1995).
- [31] E. S. Paul, H. R. Andrews, V. P. Janzen, D. C. Radford, D. Ward, T. E. Drake, J. DeGraaf, S. Pilotte, and I. Ragnarsson, *Phys. Rev. C* **50**, 741 (1994).
- [32] E. S. Paul, D. B. Fossan, K. Hauschild, I. M. Hibbert, H. Schnare, J. M. Sears, I. Thorslund, R. Wadsworth, A. N. Wilson, and J. N. Wilson, *Phys. Rev. C* **51**, R2857 (1995).
- [33] W. Satuła, R. Wyss, and F. Dönau, *Nucl. Phys.* **A565**, 573 (1993).
- [34] W. Satuła, and R. Wyss, *Phys. Scr.* **56**, 159 (1995).